Free Radical Biology and Medicine 158 (2020) 126–136

Contents lists available at ScienceDirect

Free Radical Biology and Medicine

journal homepage: www.elsevier.com/locate/freeradbiomed

Original article

The plant-derived naphthoquinone lapachol causes an oxidative stress response in *Staphylococcus aureus*

Nico Linzner[a,1], Verena Nadin Fritsch[a,1], Tobias Busche[a,b], Quach Ngoc Tung[a], Vu Van Loi[a], Jörg Bernhardt[c], Jörn Kalinowski[b], Haike Antelmann[a,*]

[a] Freie Universität Berlin, Institute of Biology-Microbiology, 14195, Berlin, Germany
[b] Center for Biotechnology, University Bielefeld, 33615, Bielefeld, Germany
[c] Institute for Microbiology, University of Greifswald, 17489, Greifswald, Germany

ARTICLE INFO

Keywords:
Staphylococcus aureus
Lapachol
Quinone
ROS
Bacillithiol
Bacilliredoxin
YpdA

ABSTRACT

Staphylococcus aureus is a major human pathogen, which causes life-threatening systemic and chronic infections and rapidly acquires resistance to multiple antibiotics. Thus, new antimicrobial compounds are required to combat infections with drug resistant *S. aureus* isolates. The 2-hydroxy-3-(3-methyl-2-butenyl)-1,4-naphthoquinone lapachol was previously shown to exert antimicrobial effects. In this study, we investigated the antimicrobial mode of action of lapachol in *S. aureus* using RNAseq transcriptomics, redox biosensor measurements, *S*-bacillithiolation assays and phenotype analyses of mutants. In the RNA-seq transcriptome, lapachol caused an oxidative and quinone stress response as well as protein damage as revealed by induction of the PerR, HypR, QsrR, MhqR, CtsR and HrcA regulons. Lapachol treatment further resulted in up-regulation of the SigB and GraRS regulons, which is indicative for cell wall and general stress responses. The redox-cycling mode of action of lapachol was supported by an elevated bacillithiol (BSH) redox potential (E_{BSH}), higher endogenous ROS levels, a faster H_2O_2 detoxification capacity and increased thiol-oxidation of GapDH and the HypR repressor *in vivo*. The ROS scavenger N-acetyl cysteine and microaerophilic growth conditions improved the survival of lapachol-treated *S. aureus* cells. Phenotype analyses revealed an involvement of the catalase KatA and the Brx/BSH/YpdA pathway in protection against lapachol-induced ROS-formation in *S. aureus*. However, no evidence for irreversible protein alkylation and aggregation was found in lapachol-treated *S. aureus* cells. Thus, the antimicrobial mode of action of lapachol in *S. aureus* is mainly caused by ROS formation resulting in an oxidative stress response, an oxidative shift of the E_{BSH} and increased protein thiol-oxidation. As ROS-generating compound, lapachol is an attractive alternative antimicrobial to combat multi-resistant *S. aureus* isolates.

1. Introduction

Staphylococcus aureus is an important human pathogen, which can cause acute skin and soft tissue infections, but also life-threatening systemic and chronic diseases, such as sepsis, endocarditis, pneumonia and osteomyelitis [1–4]. Moreover, the prevalence of multiple antibiotic resistant strains, such as methicillin-resistant *S. aureus* (MRSA) imposes a major health burden [5,6]. Thus, the discovery of new antimicrobial compounds from natural sources is an urgent need to combat infections with multi-resistant *S. aureus* isolates.

Many natural antimicrobial compounds contain quinone-like structures, such as the fungal 6-brom-2-vinyl-chroman-4-on [7]. Recently, two novel quinone compounds with cytostatic properties were discovered from the fungus *Septofusidium berolinense,* including 3,6-dihydroxy-2-propylbenzaldehyde (GE-1) and 2-hydroxymethyl-3-propylcyclohexa-2,5-diene-1,4-dione (GE-2), which act as topoisomerase-II inhibitors [8,9]. In addition, the 2-hydroxy-3-(3-methyl-2-butenyl)-1,4-naphthoquinone lapachol of the lapacho tree *Tabebuia impetiginosa* was shown to exert antimicrobial, antiparasitic and cytostatic effects [10–15]. Lapachol showed strong killing effects against various Gram-positive bacteria, such as *Bacillus subtilis*, *Enterococcus faecalis*, *Clostridium perfringens* and *S. aureus*, but was less effective against Gram-negative *Escherichia coli*, *Pseudomonas aeruginosa* and *Salmonella* Typhimurium [16–20]. Furthermore, lapachol was antiproliferative in WHCO1 oesophageal and promyelocytic leukemia HL-60 cancer cell lines with 50% growth inhibition at concentrations of 24.1 μM and

* Corresponding author. Institute of Biology-Microbiology, Freie Universität Berlin, Königin-Luise-Strasse 12-16, D-14195 Berlin, Germany.
E-mail address: haike.antelmann@fu-berlin.de (H. Antelmann).
[1] Both authors contributed equally to this work.

https://doi.org/10.1016/j.freeradbiomed.2020.07.025
Received 24 January 2020; Received in revised form 28 June 2020; Accepted 18 July 2020
Available online 24 July 2020

3.18 μM, respectively [21,22]. Cytotoxic lapachol concentrations were determined as 185 μg/ml, which kill 50% Balb/c murine peritoneal macrophages [23]. While ROS formation has been demonstrated by lapachol *in vitro* [24,25], its antimicrobial mode of action in pathogenic bacteria has not been studied in detail.

The antimicrobial and toxic effect of quinones can be attributed to their mode of actions as electrophiles and oxidants [26–31]. In the electrophilic mode, quinones lead to alkylation and aggregation of thiols via the irreversible *S*-alkylation chemistry, resulting in thiol depletion in the proteome and thiol-metabolome [29,31]. As oxidants, quinones can be reduced to semiquinone anion radicals that transfer electrons to molecular oxygen, leading to ROS formation, such as superoxide anion [24,25,27,28,32,33]. The mode of action of quinones is dependent on the physicochemical features, the chemical structure and the availability of oxygen [34–36]. In general, the toxicity and thiol-alkylation ability of quinones increases when the positions adjacent to the keto groups are unsubstituted in the quinone ring (e.g. benzoquinone) [27,34]. Fully substituted quinone rings cannot alkylate protein thiols, but retain redox-cycling activity, including ubiquinone and tetramethyl-*p*-benzoquinone [36]. Since the quinone ring is fully substituted, lapachol may act mainly via the oxidative mode as antimicrobial in *S. aureus*, which was subject of this study [27,34].

We have previously investigated the transcriptome signature in response to 2-methylhydroquinone (MHQ) in *S. aureus* [26]. MHQ was shown to induce a strong thiol-specific oxidative and quinone stress response in the *S. aureus* transcriptome [26]. The quinone-responsive QsrR and MhqR regulons were most strongly induced by MHQ and conferred independent resistance to quinones and quinone-like antimicrobials, including ciprofloxacin, pyocyanin, norfloxacin and rifampicin [26,37]. The MhqR repressor controls the *mhqRED* operon, which encodes for the predicted phospholipase/carboxylesterase MhqD and ring-cleavage dioxygenase MhqE involved in quinone detoxification [26]. The redox-sensing QsrR repressor senses quinones by thiol-*S*-alkylation and regulates paralogous dioxygenases and quinone reductases in *S. aureus* [37].

The oxidative mode of action of MHQ was revealed by induction of the peroxide-specific PerR regulon, which controls antioxidant enzymes, such as catalase and peroxidases (KatA, Tpx, Bcp), Fe-binding miniferritin (Dps) and the FeS-cluster machinery (Suf) [38–40]. Moreover, the disulfide-stress-specific HypR regulon was upregulated by MHQ, including the NADPH-dependent flavin disulfide reductase MerA [41]. In addition to ROS detoxification enzymes, *S. aureus* uses the low molecular weight thiol bacillithiol (BSH) for protection against ROS [42]. BSH is an important thiol cofactor that functions in detoxification of various redox-active compounds, electrophiles and antibiotics and contributes to survival of *S. aureus* in macrophage infection assays [42–45]. BSH also participates in redox modifications of proteins and forms protein *S*-bacillithiolation under disulfide stress, such as HOCl and the ROS-producing antimicrobial surface coating AGXX® [46–48]. Protein *S*-bacillithiolations are involved in thiol-protection and regulate protein activities as shown for the glycolytic glyceraldehyde-3-phosphate dehydrogenase (GapDH) in *S. aureus* [31,46–50]. The removal of protein *S*-bacillithiolation is controlled by bacilliredoxins (Brx), which are regenerated by BSH and the bacillithiol disulfide (BSSB) reductase YpdA [48,51–53]. Moreover, the Brx/BSH/YpdA pathway is important for protection of *S. aureus* under oxidative stress and infection conditions [51,52].

In this study, we analyzed the molecular stress responses and mode of action of lapachol in *S. aureus*. Using RNA-seq transcriptomics, lapachol induced an oxidative and quinone stress response as well as strong protein damage in *S. aureus*. This signature was revealed by the induction of the QsrR, MhqR, PerR, HypR, CtsR and HrcA regulons and of the enzymes of the Brx/BSH/YpdA redox pathway. The oxidative mode of action of lapachol was demonstrated by an oxidative shift of the BSH redox potential, elevated ROS formation and faster H_2O_2 detoxification capacity, increased protein *S*-bacillithiolation of GapDH and thiol-oxidation of the HypR repressor *in vivo*. However, no evidence for protein alkylation and aggregation was revealed. In support of the oxidative mode, the ROS scavenger N-acetyl cysteine and microaerophilic growth conditions improved the survival of *S. aureus* under lapachol stress. Phenotype analyses revealed that KatA and the Brx/BSH/YpdA pathway are important for the defense of *S. aureus* against lapachol-induced ROS. Overall, our results indicate that the antimicrobial effect of lapachol is mainly caused by ROS-formation, resulting in an impaired redox homeostasis and increased protein thiol-oxidation in *S. aureus*.

2. Experimental procedures

Bacterial strains, growth and survival assays. For cloning and genetic manipulation, *E. coli* was cultivated in Luria broth (LB) medium. The His-tagged GapDH protein of *S. aureus* was expressed and purified in *E. coli* BL21(DE3) *plys*S with plasmid pET11b-*gapDH* as previously described [48]. For lapachol stress experiments, we used *S. aureus* COL *katA*, *bshA*, *brxAB* and *ypdA* deletion mutants and the *katA, bshA*, *ypdA, brxA* and *brxB* complemented strains as described in Tables S1 and S2 [51]. *S. aureus* strains were cultivated in LB, RPMI or Belitsky minimal medium (BMM) depending on the specific experiments and treated with lapachol during the exponential growth as described [41,54]. Specifically, biosensor experiments, *S*-bacillithiolation and HypR oxidation assays were performed in BMM medium due to high expression of the biosensor and low ROS quenching effects as described [54,55]. All growth and survival assays as well as RNA-seq experiments were performed in rich RPMI medium, which resembles infection conditions and allows fast growth. Survival assays were performed by plating 100 μl of serial dilutions of *S. aureus* onto LB agar plates and determination of colony forming units (CFUs). Statistical analysis was performed using Student's unpaired two-tailed *t*-test by the graph prism software. Lapachol, diamide, sodium hypochlorite (NaOCl), N-acetyl cysteine, dithiothreitol (DTT) and cumene hydroperoxide (CHP, 80% w/v) were purchased from Sigma Aldrich.

Determination of the minimal inhibitory concentration (MIC) of lapachol. MIC assays were performed in 96-well plates with 200 μl of serial two-fold dilutions of the 40 mM lapachol stock in RPMI medium. The *S. aureus* overnight culture was inoculated to an OD_{500} of 0.03 into the microplate wells. After 24 h shaking at 37 °C, the OD_{500} was measured using the CLARIOstar microplate reader (BMG Labtech).

Construction of *S. aureus* COL *katA* and *bshA* mutants as well as complemented strains. The construction of the *S. aureus katA* and *bshA* deletion mutants was performed using the pMAD *E. coli/S. aureus* shuttle vector as described [41,56]. Briefly, the 500 bp up- and downstream regions of *katA* and *bshA* were amplified using primers pMAD-katA-for-BglII, pMAD-katA-f1-rev, pMAD-katA-f2-for, pMAD-katA-rev-SalI for *katA* and pMAD-bshA-f1-rev, pMAD-bshA-for-BglII, pMAD-bshA-rev-SalI, pMAD-bshA-f2-for for *bshA* (Table S3), fused by overlap extension PCR and ligated into the *Bgl*II and *Sal*I sites of plasmid pMAD. The pMAD constructs were electroporated into *S. aureus* RN4220 and further transduced into *S. aureus* COL using phage 81 [57]. The clean deletions of *katA* and *bshA* were selected after plasmid excision as described [41].

For construction of the *katA* and *bshA* complemented strains, the xylose-inducible ectopic *E. coli/S. aureus* shuttle vector pRB473 was applied [58]. Primer pairs pRB-katA-for-*Bam*HI and pRB-katA-rev-*Kpn*I as well as pRB-bshA-for-*Bam*HI and pRB-bshA-rev-*Kpn*I (Table S3) were used for amplification of *katA* and *bshA*, respectively. The PCR products were cloned into pRB473 after digestion with *Bam*HI and *Kpn*I to generate plasmids pRB473-*katA* and pRB473-*bshA*. The pRB473-*katA* and pRB473-*bshA* plasmids were transduced into the *katA* and *bshA* deletion mutants, respectively, to construct the complemented strains as described [54].

For construction of *S. aureus* COL WT expressing His-tagged HypR, *hypR*-His was amplified from the *S. aureus* COL genome by PCR using

primer pRB-hypR-for-BamHI and primer pRB-hypR-His-rev-KpnI (Table S3), which included the codons for 6 His residues at the C-terminus. The PCR product was cloned into plasmid pRB473 after digestion with *Bam*HI and *Kpn*I to generate plasmid pRB473-*hypR*-His, which was introduced into *S. aureus* COL WT via phage transduction as described [41].

Live/Dead viability assay. The viability assay of *S. aureus* COL WT was conducted after treatment with sub-lethal and lethal concentrations of 0.3–1 mM lapachol at an OD_{500} of 0.5 using the LIVE/DEAD™ BacLight™ bacterial viability kit (Thermo Fisher) as described [59]. In brief, *S. aureus* COL was stained with SYTO9 or propidium iodide for live or dead cells, respectively. Fluorescence was analyzed after excitation at 488 and 555 nm using a fluorescence microscope (Nikon, Eclipse, T*i*2) (SYTO9 Ex: 488 nm, propidium iodide Ex: 555 nm). Live and dead cells were false-colored in green and red, respectively.

RNA isolation, library preparation, next generation cDNA sequencing and differential gene expression analysis after lapachol stress. RNA-seq transcriptomics was performed using RNA of *S. aureus* COL, which was grown in RPMI medium and subjected to 0.3 mM lapachol for 30 min as described [59]. Differential gene expression analysis of 3 biological replicates was performed using DESeq2 [60] with ReadXplorer v2.2 [61] using an adjusted p-value cut-off of $P \leq 0.05$ and a signal intensity ratio (M-value) cut-off of ≥ 1 or ≤ -1 (fold-change of $\pm$ 2) as described previously [59]. The RNA-seq raw data files for the whole transcriptome are available in the ArrayExpress database (www.ebi.ac.uk/arrayexpress) under E-MTAB-8691.

Construction of the Voronoi transcriptome treemap. The lapachol transcriptome treemap was constructed using the Paver software (DECODON GmbH, Greifswald, Germany) as described [59]. The red-blue color gradient indicates log2-fold changes (M-values) of selected genes, operons and regulons that are up- or down-regulated under lapachol stress. The cell sizes denote absolute log2-fold changes in the transcriptome under lapachol versus the control.

Brx-roGFP2 and Tpx-roGFP2 biosensor measurements. *S. aureus* COL expressing the biosensor plasmids pRB473-*tpx-roGFP2* and pRB473-*brx-roGFP2* were grown in LB overnight and used for measurements of the biosensor oxidation degree (OxD) after treatment with 100 µM lapachol as described [51,54]. The fully reduced and oxidized controls of *S. aureus* cells expressing Tpx-roGFP2 were treated with 15 mM DTT and 20 mM cumene hydroperoxide, respectively. The Brx-roGFP2 and Tpx-roGFP2 biosensor fluorescence emission was measured at 510 nm after excitation at 405 and 488 nm using the CLARIOstar microplate reader (BMG Labtech). The OxD of the Brx-roGFP2 and Tpx-roGFP2 biosensors was determined for each sample and normalized to fully reduced and oxidized controls as described [51,54].

Analyses of GapDH *S*-bacillithiolation and thiol-oxidation of the HypR repressor after lapachol stress. For GapDH *S*-bacillithiolation assay *in vivo*, *S. aureus* cells were grown in LB until an OD_{540} of 2, harvested by centrifugation and transferred to Belitsky minimal medium (BMM) as described [47]. The cells were treated with 100 µM lapachol and harvested after 30, 60, 120 and 180 min in TE buffer (pH 8.0) with 50 mM N-ethylmaleimide (NEM). Protein extracts were prepared and analyzed by BSH-specific Western blot analysis for *S*-bacillithiolated proteins using polyclonal rabbit anti-BSH antiserum as described [47]. To analyze *S*-bacillithiolation of purified GapDH with lapachol *in vitro*, 60 µM of GapDH was *S*-bacillithiolated with 600 µM BSH in the presence of 10-fold excess of 6 mM lapachol for 5 min. As control, GapDH was incubated with BSH in the absence of lapachol. Excess of BSH and lapachol were removed with Micro Biospin 6 columns (Biorad). *S*-bacillithiolation of GapDH was analyzed using non-reducing BSH-specific Western blots. To study thiol-oxidation of the HypR repressor *in vivo*, *S. aureus* COL WT strain expressing His-tagged HypR (Table S1) was cultivated as described for the *in vivo S*-bacillithiolation assay above. Cell extracts were alkylated with 50 mM NEM and HypR oxidation analyzed using non-reducing SDS-PAGE and Western blot analysis with His-tag specific monoclonal antibodies (Thermo Fisher).

Analysis of H_2O_2 detoxification capacity in cell extracts by the FOX assay. The FOX assay was performed with cytoplasmic cell extracts as described previously [62]. FOX reagent was prepared by adding 100 ml FOX I (100 mM sorbitol, 125 µM xylenol orange) to 1 ml FOX II (25 mM ammonium ferrous(II)sulfate in 2.5 M H_2SO_4). To prepare cytoplasmic extracts, *S. aureus* COL WT was cultivated in RPMI to an OD_{500} of 0.5, exposed to 0.3 mM lapachol and harvested after 1 h and 2 h. Cells were washed in 83 mM phosphate buffer (pH 7.05), disrupted using the ribolyzer and 100 µl cell lysate was added to 500 µl of 10 mM H_2O_2 solution. After different times (1–5 min), 2 µl of the samples were added to 200 µl FOX reagent and incubated for 30 min at room temperature. The absorbance was measured at 560 nm using the CLARIOstar microplate reader. H_2O_2 standard curves were measured with 20 µl H_2O_2 (0–18 µM final concentrations) and 200 µl FOX reagent as above.

Protein aggregation assays after lapachol stress *in vitro* and *in vivo*. For *in vitro* aggregation analyses, purified GapDH was pre-reduced with 10 mM DTT for 30 min at RT and DTT was removed with spin columns. Subsequently, 5 µM GapDH was incubated with different concentrations of lapachol for 30 min at RT and subjected to SDS-PAGE. For isolation of insoluble protein aggregates of cell extracts *in vivo*, *S. aureus* COL WT was cultivated in RPMI to an OD_{500} of 0.5 and treated with 0.3 and 1.0 mM lapachol for 30 min. Cell extracts were harvested and protein aggregates isolated as insoluble protein fraction as described previously [59,63,64].

3. Results

Lapachol has a strong antimicrobial and killing effect in *S. aureus* COL. To determine the growth-inhibitory and lethal lapachol concentrations, *S. aureus* COL was grown in RPMI medium and exposed to increasing doses 0.3–1 mM lapachol during the exponential growth (Fig. 1A,B). Cell viability was analyzed using CFU counting and the LIVE/DEAD™ Bacterial Viability Kit (Fig. 1B,C). Sub-lethal doses of 0.3 mM lapachol resulted in a decreased growth rate, but cells were able to recover in growth and the survival rate was not affected (Fig. 1A,B). This result was confirmed using live/dead staining since only few red cells were observed after treatment with sub-lethal 0.3 mM lapachol similar as in the untreated control (Fig. 1C). Increasing concentrations of 0.4–1 mM lapachol were lethal for *S. aureus* COL as shown by decreased growth and viability rates (Fig. 1A,B). Only few SYTO9-labelled cells could be observed using the LIVE/DEAD™ assay after exposure to 0.7–1 mM lapachol, indicating that lapachol exerts a strong antimicrobial and killing effect in *S. aureus* (Fig. 1C). However, the MIC of lapachol was determined as 1.25 mM in *S. aureus* (Table S4), which was higher compared to the growth-inhibitory amount. The higher MIC is probably caused by inactivation of lapachol over the long time of incubation for 24 h in the microplate assay.

Lapachol induces a quinone and oxidative stress response in the *S. aureus* COL transcriptome. In previous transcriptome studies, we monitored physiological stress responses by treatment of *S. aureus* with sub-lethal doses of antimicrobial compounds [41,59,65]. Thus, the changes in the transcriptome were analyzed after exposure of *S. aureus* COL to sub-lethal 0.3 mM lapachol stress for 30 min in 3 biological replicates using the RNA-seq method as described earlier [41]. Significant differential gene expression is indicated by the M-value cut-off (log2-fold change lapachol/control) of ≥ 1 and ≤ -1 (fold-change of $\pm$ 2, $P \leq 0.05$) which includes most known redox regulons up-regulated under lapachol stress (Fig. 2). In total, 564 genes were significantly > 2-fold up-regulated and 515 genes were < -2-fold down-regulated in the lapachol transcriptome of *S. aureus* COL (Fig. 2, Tables S5 and S6). Overall, the significantly and most strongly induced regulons in the lapachol transcriptome include the CtsR, HrcA, PerR, HypR, NsrR, MhqR, QsrR, CymR, SaeRS, GraRS and SigB regulons. These regulons indicate that lapachol causes an oxidative and quinone

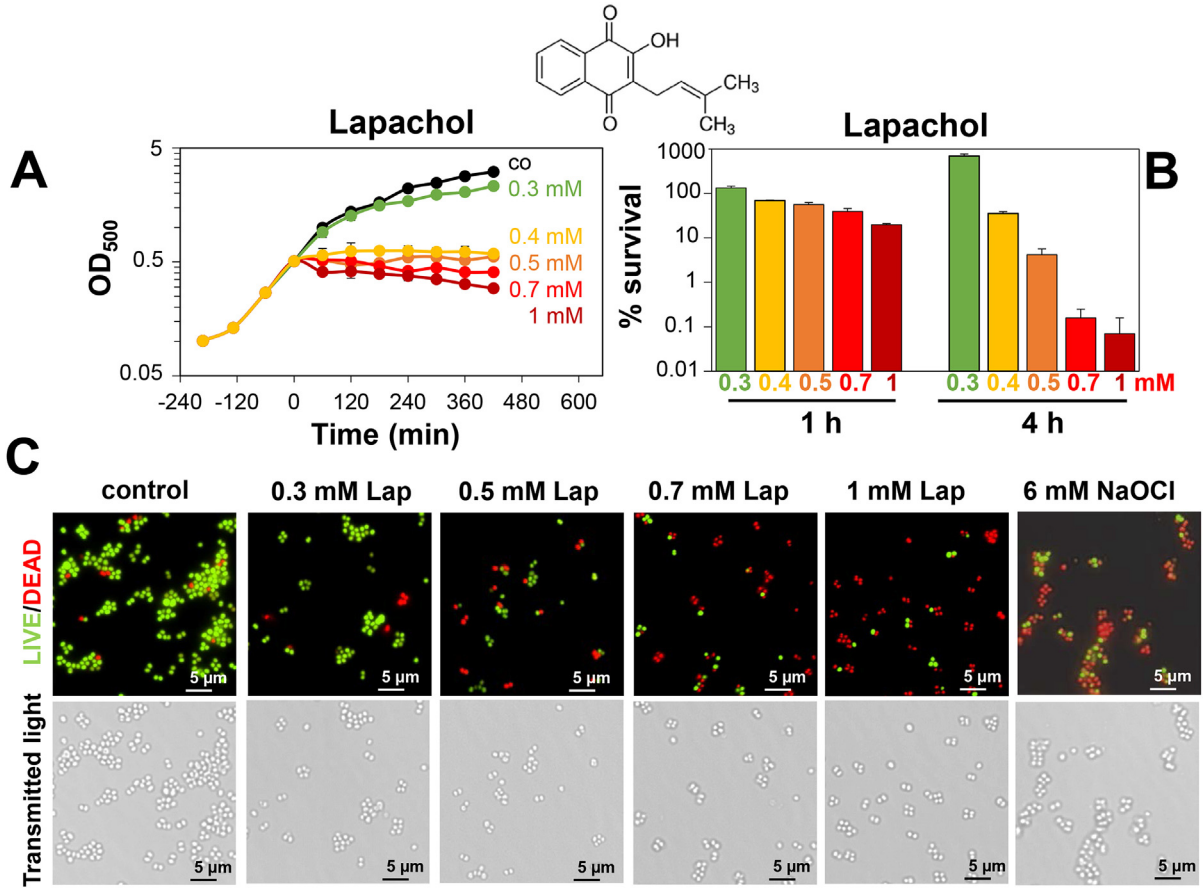

Fig. 1. Lapachol has a strong antimicrobial effect in *S. aureus*. (A–C) The structure of the 2-hydroxy-3-(3-methyl-2-butenyl)-1,4-naphthoquinone lapachol is shown above the figures **(A)** and **(B)**. *S. aureus* COL was grown in RPMI medium to an OD_{500} of 0.5 and exposed to sub-lethal (300 µM) and lethal (0.4, 0.5, 0.7 and 1 mM) doses lapachol. **(A)** Growth curves and **(B)** survival assays were performed to determine sub-lethal and lethal lapachol concentrations. The cells were plated for CFUs after 1 and 4 h of lapachol stress. **(C)** Cell viability was also analyzed after 1 h of lapachol stress using the Live/Dead™ BacLight™ Bacterial Viability Kit and visualized with a fluorescence microscope (Nikon, Eclipse, Ti2). Live and dead cells show green and red fluorescence, respectively. As control for dead cells, the toxic concentration of 6 mM NaOCl was applied.

stress transcriptome signature and protein damage. Up-regulated genes and regulons are labelled with different color codes in the ratio/intensity scatter plot (M/A-plot) and are also displayed in the Voronoi transcriptomics treemap (Figs. 2 and 3, Tables S5 and S6).

Lapachol stress leads to strong induction of the CtsR and HrcA regulons, which control the protein quality control machinery, including Clp proteases and the DnaK-GrpE, GroESL chaperones [66,67]. The heat-shock specific CtsR controlled *ctsR-mcsA-mcsB-clpC* operon and the HrcA-regulated *hrcA-grpE-dnaKJ* operon are 46-62-fold and 44-50-fold up-regulated, respectively, under lapachol stress (Figs. 2 and 3, Tables S5 and S6). Thus, lapachol induces strong protein damage, which might be caused by oxidative or electrophilic protein modifications, such as thiol-oxidation or *S*-alkylations. Among the top scorers was further the peroxide specific PerR regulon with fold-changes of 5–26. The PerR-regulon genes encode for peroxidases *ahpCF* (20-26-fold), *bcp* (11-fold), *tpx* (5-fold), the catalase *katA* (11-fold), the mini-ferritin *dps* (11-fold) and the thioredoxin reductase *trxB* (5-fold) (Figs. 2 and 3, Tables S5 and S6). The induction of the PerR-regulon confirms that lapachol acts via the oxidative mode leading to ROS formation, such as H_2O_2 inside *S. aureus*. Furthermore, both genes encoding superoxide dismutases (*sodA1* and *sodA2*) were highly expressed (11-12-fold) under lapachol stress (Fig. 2, Tables S5 and S6). This supports the generation of superoxide anions in the oxidative mode of lapachol as has been measured previously *in vitro* [24].

In addition, lapachol resulted in 23-26-fold induction of the NsrR-controlled *hmp* gene encoding a flavohemoglobin, which is predominantly involved in nitric oxide detoxification [68]. Interestingly, Hmp of *S. aureus* was shown to function in quinone and nitrocompound detoxification using mixed one- and two electron reduction mechanisms [69]. Hmp exhibits a strong substrate preference for 2-methyl-1,4-naphthoquinones [69], which are related to lapachol. Thus, Hmp might be involved in lapachol detoxification in *S. aureus*. Furthermore, the HypR regulon, including the disulfide reductase encoding *merA* gene was 5-fold induced by lapachol, which is indicative for disulfide stress caused by lapachol [41].

The RNA-seq transcriptome data further suggest an electrophilic mode of action of lapachol, as revealed by the significant induction of both quinone-specific MhqR and QsrR regulons. The MhqR-regulated *mhqRED* operon was 10-fold induced under lapachol treatment. The QsrR regulon genes encoding quinone reductases and dioxygenases are 3.7-9-fold up-regulated by lapachol, including *catE, catE2*, *azoR1*, *frp* and *yodC* (Figs. 2 and 3, Tables S5 and S6). Thus, the main transcriptome signature suggests that lapachol exerts its toxicity as oxidant and electrophile in *S. aureus*. In addition, lapachol leads to strong up-regulation of the SaeRS, GraRS and SigB regulons. Among the virulence factor controlling SaeRS regulon, the myeloperoxidase inhibitor SPIN was most strongly 123-fold induced, while the γ-hemolysin operon *hlgABC* was 8-10-fold up-regulated by lapachol. Several GraRS regulon members were 3-60-fold up-regulated. The large GraRS regulon responds to cell wall-active antibiotics and is involved in the oxidative stress defense in *S. aureus* [70]. Finally, the genes encoding enzymes for biosynthesis of BSH and the Brx/YpdA pathway, such as *bshA*, *bshB*,

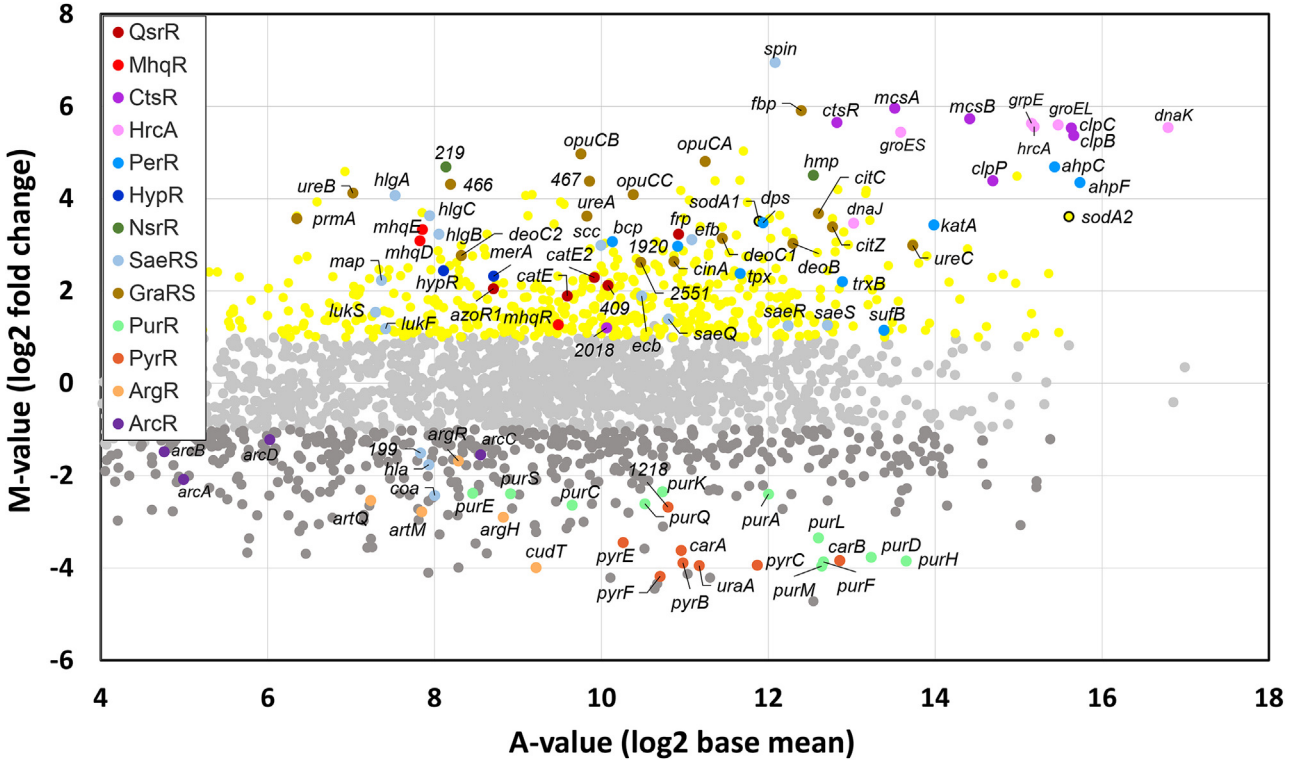

Fig. 2. RNA-seq transcriptomics after lapachol stress in *S. aureus* COL. For RNA-seq transcriptomics, *S. aureus* COL was grown in RPMI medium and treated with 300 μM lapachol for 30 min. The gene expression profile is shown as ratio/intensity scatter plot (M/A-plot) which is based on differential gene expression analysis using DeSeq2. Colored symbols indicate subsets of the significantly induced regulons QsrR, MhqR, CtsR, HrcA, PerR, HypR, SaeRS, NsrR (dark red, red, magenta, light magenta, blue, dark blue, light blue, green). The significantly down-regulated regulons PurR, PyrR, ArgR, ArcR are labelled in light green, orange, light orange and dark violet. All other significantly induced (yellow) or repressed (dark grey) transcripts were defined with an M-value ≥ 1 or ≤ -1; P-value ≤ 0.05. Light grey symbols denote transcripts with no fold-changes after lapachol stress (P > 0.05). The transcriptome analysis was performed from three biological replicates. The RNA-seq expression data of all genes after lapachol stress and their regulon classifications are listed in Tables S5 and S6.

bshC, brxB and *ypdA* were 2-4-fold up-regulated by lapachol in *S. aureus*. This further points to the generation of ROS in the oxidative mode of lapachol resulting in an impaired redox homeostasis in *S. aureus*.

Among the down-regulated regulons, the CodY and ArgR regulons involved in the biosynthesis of branched chain amino acids (lysine, isoleucine and leucine) and arginine, respectively, were strongly repressed in the lapachol transcriptome. The PyrR and PurR regulons, which control purine and pyrimidine biosynthesis operons were further down-regulated under lapachol. The shut-down of amino acid and nucleotide biosynthesis enzymes might be caused by decreased ATP levels since the ATP synthase operon was further down-regulated under lapachol stress (Figs. 2 and 3, Tables S5 and S6).

Altogether, the RNA-seq transcriptome signature indicates that lapachol causes an oxidative, quinone and cell wall stress response as well as protein damage, suggesting its mode of action as oxidant and electrophile.

Lapachol stress leads to an increased BSH redox potential, elevated endogenous ROS levels and enhanced H_2O_2 detoxification in *S. aureus*. Previous studies revealed that lapachol is reduced to its semiquinone anion radical, leading to reduction of O_2 and formation of reactive oxygen species (ROS), such as superoxide anions and hydroxyperoxyl radicals [24,25]. Our transcriptome data further support the oxidative mode of lapachol and an impaired redox balance (Figs. 2 and 3). Thus, we applied the recently constructed genetically encoded Brx-roGFP2 and Tpx-roGFP2 biosensors to measure intracellular redox changes in *S. aureus* after sub-lethal doses of 100 μM lapachol [51,54]. The coupled Brx-roGFP2 biosensor is specific for BSSB leading to *S*-bacillithiolation of the Brx active site Cys and transfer of BSH to the roGFP2 moiety, which finally rearranges to the roGFP2 disulfide [54]. Oxidation of roGFP2 results in a ratiometric change of the 405 and 488 nm excitation maxima. The 405/488 nm excitation ratio of Brx-roGFP2 after lapachol stress reflects the oxidation degree (OxD) of the biosensor and the changes in the BSH redox potential (E_{BSH}) in *S. aureus* [54]. The Brx-roGFP2 biosensor showed an increased OxD of 0.65 after 100 μM lapachol stress compared to the untreated control (OxD ~ 0.3) (Fig. 4A). However, cells were unable to regenerate the reduced basal level of E_{BSH} within 3 h of lapachol stress. These results indicate that lapachol causes a constant oxidative shift in E_{BSH} in *S. aureus* probably due to its redox-cycling action.

Next, we monitored endogenous H_2O_2 levels using the Tpx-roGFP2 biosensor in *S. aureus* after lapachol stress [51]. The Tpx-roGFP2 biosensor is specific for low levels of H_2O_2 [51]. H_2O_2 reacts with the Tpx active site to Cys sulfenic acid (SOH), which is transferred to roGFP2 leading to roGFP2 disulfide formation and the ratiometric changes in the roGFP2 excitation spectrum. The Tpx-roGFP2 biosensor was shown to respond very fast to 100 μM lapachol leading to an increased OxD of ~0.7 (Fig. 4B). These results confirm that lapachol treatment leads to increased endogenous H_2O_2 levels resulting in an increased E_{BSH} supporting the oxidative mode of action. In addition, the FOX assay was performed to investigate the H_2O_2 detoxification capacity of cellular extracts of *S. aureus* after lapachol stress. H_2O_2 detoxification occurred much faster in lapachol-treated cell extracts, compared to that of untreated control cells (Fig. 4C). Thus, *S. aureus* has an enhanced H_2O_2 detoxification capacity after lapachol stress due to a higher catalase activity, which is consistent with the increased expression of the PerR controlled *katA* and *ahpCF* antioxidant genes.

The ROS scavenger N-acetyl cysteine and microaerophilic growth conditions improve the survival of *S. aureus* under lapachol stress. Since ROS generation by lapachol depends on oxygen

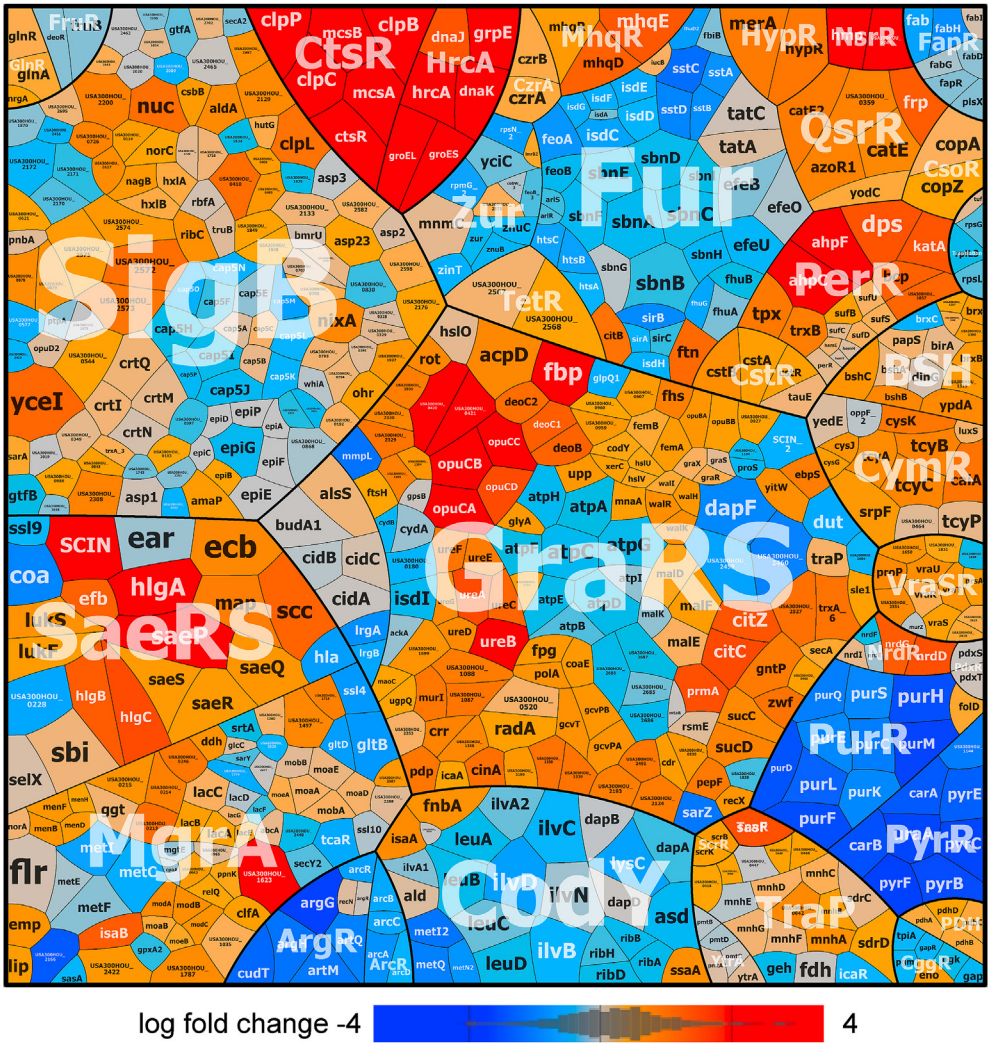

Fig. 3. The transcriptome treemap after lapachol indicates an oxidative and quinone stress response in *S. aureus* COL. The treemap shows the log2-fold changes (M-values) using the red-blue color code where red indicates log2-fold induction and blue repression of selected regulons after exposure to 300 μM lapachol in the RNA-seq transcriptome of *S. aureus* COL. The genes, operons and regulons are based on RegPrecise (http://regprecise.lbl.gov/RegPrecise/index.jsp) and previous classifications. Lapachol caused a strong quinone and oxidative stress response as well as protein damage as revealed by induction of the PerR, HypR, QsrR, MhqR, CtsR, HrcA regulons in *S. aureus*. The induction of the SigmaB and GraRS regulons further indicates cell wall and general stress responses in *S. aureus*. The detailed transcriptome data of all genes differentially expressed in response to lapachol are presented in Tables S5 and S6.

availability, we compared the survival of *S. aureus* under aerobic and microaerophilic growth conditions. The results showed that the survival of *S. aureus* was strongly improved after 0.4 and 1 mM lapachol stress under microaerophilic conditions (Fig. 5A). Both concentrations were lethal under aerobic conditions (Fig. 1B; Fig. 5A). While microaerophilic growth resulted in ~80% survival of cells exposed to 1 mM lapachol, only less than 1% of cells survived with 1 mM lapachol under aerobic conditions (Fig. 5A). This result was supported by the ROS scavenger N-acetyl cysteine, which was added to the aerobic culture before the exposure to 0.4 mM lapachol (Fig. 5B). The aerobic *S. aureus* culture treated with N-acetyl cysteine showed significantly improved survival after 0.4 mM lapachol stress (Fig. 5B). Together, our results revealed that the antimicrobial effect of lapachol is based on ROS formation, since decreased ROS levels lead to an enhanced survival of lapachol-treated cells.

Lapachol causes increased *S*-bacillithiolation of GapDH and thiol-oxidation of the HypR repressor in *S. aureus*. Previously, we used BSH-specific Western blots to analyze the extent of protein *S*-bacillithiolation in *S. aureus* under HOCl stress [48]. The glyceraldehyde-3-phosphate dehydrogenase GapDH was the most abundant *S*-bacillithiolated protein under HOCl stress that could be visualized as major band in non-reducing BSH-specific Western blots [48]. Thus, we investigated the oxidative mode of action of lapachol by analysis of the pattern of *S*-bacillithiolation in *S. aureus*. The BSH specific Western blots revealed an increased *S*-bacillithiolation of the GapDH band after 30–120 min of lapachol stress, which was absent in the *bshA* mutant (Fig. 6A). These results confirm the oxidative mode of action to induce thiol-oxidation of GapDH in *S. aureus in vivo*.

Next, we used BSH-specific non-reducing Western blots to investigate whether lapachol-induced ROS can also lead to *S*-bacillithiolation of purified GapDH *in vitro*. Pre-reduced GapDH was treated with lapachol in the presence of BSH. While no *S*-bacillithiolated GapDH band was visible in the control reaction of GapDH with BSH alone, the presence of lapachol strongly induced *S*-bacillithiolation of GapDH *in vitro* (Fig. 6B). However, we did not find evidence for protein alkylation or aggregation of purified GapDH after treatment with increasing doses 0.5–7.5 mM lapachol alone as revealed by SDS-PAGE (Fig. S1A). In addition, we isolated the insoluble protein fraction of protein aggregates from lapachol-treated cells using the protocol as established previously [63,64]. However, the results did not reveal increased protein aggregates after lapachol stress (Fig. S1B).

To further support the oxidative mode of lapachol, we investigated the redox state of the redox-sensing HypR repressor, which senses disulfide stress by intersubunit disulfide formation in *S. aureus* [41]. *S. aureus* cells expressing His-tagged HypR protein were subjected to different concentrations of 0.1–1 mM lapachol stress. The redox state of HypR was analyzed using non-reducing Western blots with anti-His-tag specific monoclonal antibodies. The results revealed that lapachol leads to oxidation of HypR to the intermolecular disulfide-linked dimer after lapachol stress (Fig. S2AB). Thiol-oxidation of HypR was reversible with DTT, supporting the oxidative mode of lapachol. However, we could not detect irreversible protein alkylation and aggregation of

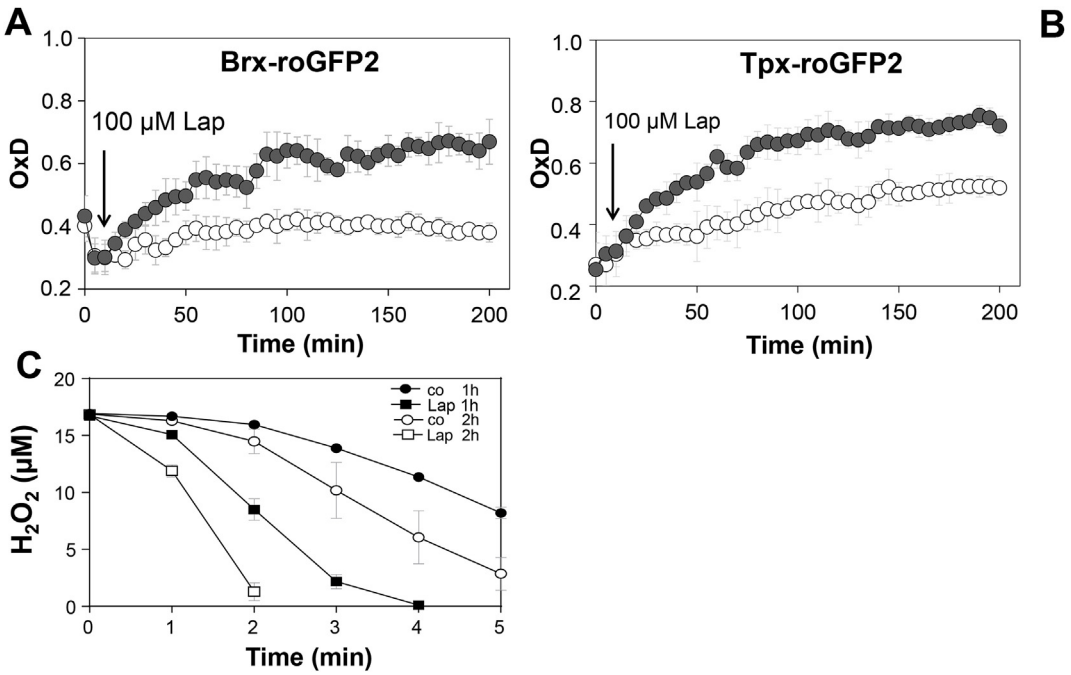

Fig. 4. Lapachol causes an increased BSH redox potential, elevated endogenous H_2O_2 levels and faster H_2O_2 detoxification in *S. aureus* COL. Responses of the Brx-roGFP2 **(A)** and Tpx-roGFP2 **(B)** biosensors to 100 µM lapachol stress in *S. aureus* COL. The oxidation degrees (OxD) of the Brx-roGFP2 and Tpx-roGFP2 biosensors were calculated for untreated control cells (white symbols) and after lapachol stress (grey symbols). OxD values were calibrated to fully reduced and oxidized controls. **(C)** Lapachol-treated *S. aureus* cells showed faster H_2O_2 detoxification in the FOX assay indicating higher catalase activity. *S. aureus* was exposed to 0.3 mM lapachol for 1–2 h and cell extracts were analyzed for H_2O_2 decomposition using the FOX-Assay. Mean values and SD of 3–4 biological replicates are shown.

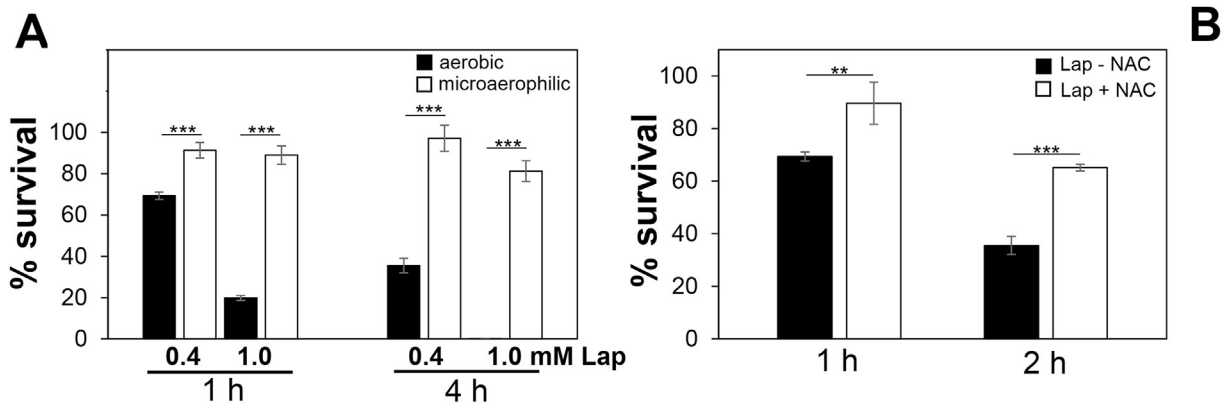

Fig. 5. Microaerophilic growth and the ROS-scavenger N-acetyl cysteine improve survival of *S. aureus* under lapachol stress. (A) Survival assays were performed of *S. aureus* COL WT grown in RPMI under aerobic or microaerophilic conditions after exposure to 0.4 and 1 mM lapachol at an OD_{500} of 0.5. The aerobic survival rates are the same shown in Fig. 1B. **(B)** Survival rates were determined under aerobic growth conditions after 0.4 mM lapachol stress in the absence or presence of 1.25 mM N-acetyl cysteine (NAC). CFUs were determined after 1 or 4 h of stress exposure and the survival of the untreated control was set to 100%. Mean values and SD of three to four biological replicates are presented. The statistics was calculated using a Student's unpaired two-tailed *t*-test by the graph prism software. Symbols are: $^{**}p \leq 0.01$ and $^{***}p \leq 0.001$.

proteins in the Western blot or SDS-PAGE loading control. Together, our results support the oxidative mode of lapachol to induce protein *S*-bacillithiolation of GapDH *in vitro* and *in vivo* as well as reversible thiol-oxidation of the redox-sensing HypR repressor in *S. aureus*.

The catalase KatA and the Brx/BSH/YpdA pathway confer tolerance of *S. aureus* towards lapachol treatment. To confirm the oxidative mode of lapachol by ROS generation, we analyzed the phenotype of the *katA* mutant deficient for the major catalase. The *katA* mutant displayed a growth delay under lapachol stress and was strongly impaired in survival compared to the parent (Fig. 7A,B). These results clearly confirm the production of H_2O_2 and increased catalase activity by lapachol as shown with the Tpx-roGFP2 biosensor and FOX assay, since the *katA* mutant is very sensitive to oxidative stress. In addition, we showed previously that the BrxA/BSH/YpdA redox pathway is important for de-bacillithiolation of proteins during recovery from oxidative stress and infection conditions [51]. Here, we have shown that lapachol causes an oxidative shift in E_{BSH} and increased *S*-bacillithiolation of GapDH (Figs. 4 and 6). Thus, we investigated the phenotypes of the *bshA*, *brxAB* and *ypdA* deletion mutants during growth and survival of *S. aureus* under lapachol stress. The growth of mutants deficient for BSH, bacilliredoxins BrxA/B and the BSSB reductase YpdA was significantly impaired after exposure to sub-lethal 0.3 mM lapachol (Fig. 7C,E,G). Furthermore, all mutants showed a significantly decreased survival after lethal 0.4 mM lapachol stress (Fig. 7D,F,H). These lapachol-sensitive phenotypes could be restored back to WT level after complementation with *katA*, *bshA*, *brxA* and *ypdA*, respectively (Fig. 7B,D,F,H; Fig. S3A,B,C,E). However, the complementation of the *brxAB* mutant with *brxB* did not restore the

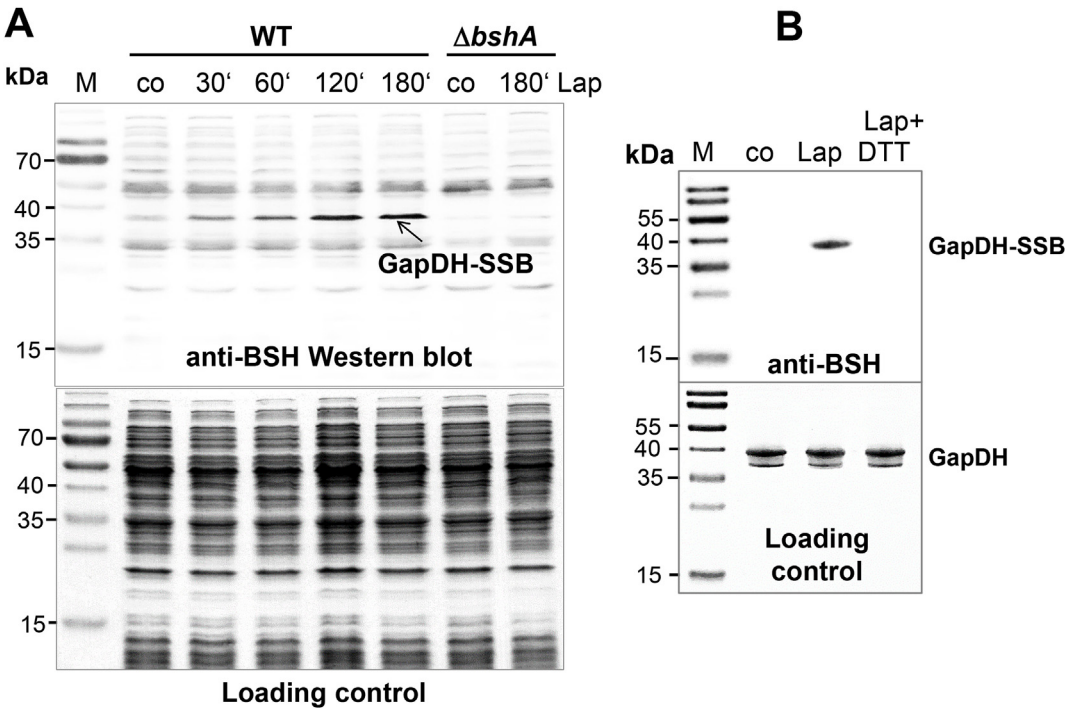

Fig. 6. Lapachol leads to *S*-bacillithiolation of GapDH *in vivo* and *in vitro*. (A) *S. aureus* COL WT and the *bshA* mutant were exposed to 100 μM lapachol for different times and the *S*-bacillithiolated GapDH (GapDH-SSB) is visualized in BSH-specific Western blot as most abundant *S*-bacillithiolated protein as shown previously under NaOCl stress [48]. **(B)** Purified GapDH is treated with 6 mM lapachol in the presence of 600 μM BSH resulting in *S*-bacillithiolation of GapDH *in vitro* as revealed in BSH-specific Western blots. As control, GapDH was treated with BSH alone (co). The Coomassie-stained SDS-PAGE loading controls are shown below the BSH Western blots.

phenotype back to wild type level (Fig. 7H; Fig.S3D). Taken together, these results revealed that the catalase KatA and the BrxA/BSH/YpdA redox pathway provide protection against lapachol-induced ROS formation in *S. aureus*.

4. Discussion

In this study, we have analyzed the antimicrobial mode of action of the naphthoquinone lapachol in the major pathogen *S. aureus*. Using growth and survival assays, the sub-lethal lapachol concentration was determined as 0.3 mM, while higher doses of 0.4–1.0 mM were toxic for *S. aureus* and strongly decreased the survival. Previously, the MIC of lapachol in *S. aureus* has been determined as 128–256 μg/ml (~0.53–1.06 mM) [71], which is in agreement with the MIC determined in this work. Since low doses of 0.4 mM lapachol are toxic for exponentially growing *S. aureus* cells, lapachol could be suited as redox-active antimicrobial to treat MRSA strains in wound infections.

In this work, we combined RNA-seq transcriptomics, redox biosensor measurements, protein thiol-oxidation assays and phenotype analyses of mutants to investigate the antimicrobial mode of action and stress responses caused by lapachol in *S. aureus*. The transcriptome results showed that lapachol caused an oxidative and quinone stress response and protein damage in *S. aureus*. The oxidative stress-specific PerR and HypR regulons, which control catalases, peroxidases and disulfide reductases, and the superoxide dismutases *sodA1* and *sodA2* are most strongly up-regulated by lapachol, which are indicative for the oxidative mode of action of lapachol. This antioxidant response induced by lapachol supports the generation of ROS by the redox cycling action of lapachol, such as superoxide anions, which are converted to H_2O_2 by SodA1/2.

Thus, our results are in agreement with previous studies of the bioactivation of lapachol using NADPH-dependent cytochrome P450 reductase and the interaction of lapachol with oxygen *in vitro* [24,25]. The naphthoquinone lapachol was shown to be bioactivated via reduction by P450 reductase to semiquinone anion radical, which leads to electron transfer to molecular oxygen, resulting in superoxide anion generation [25]. In an electrochemical study, the semiquinone anion radical was demonstrated to interact with oxygen in an electron-chain mechanism, resulting in the deprotonated lapachol and hydroxyperoxyl radicals [24].

To investigate the oxidative stress response caused by lapachol-induced ROS, we studied the changes of the BSH redox potential and endogenous H_2O_2 formation by lapachol using the Brx-roGFP2 and Tpx-roGFP2 biosensors in *S. aureus*. Our results showed an oxidative shift of E_{BSH} after lapachol stress in *S. aureus*. Increased H_2O_2 production was measured in *S. aureus* with the Tpx-roGFP2 biosensor after lapachol exposure. However, both biosensors could not be regenerated after 3 h of stress, which is probably caused by the constant redox-cyclic action of lapachol in *S. aureus*. In addition, we used the FOX assay to demonstrate an enhanced H_2O_2 detoxification capacity of *S. aureus* cells after lapachol stress, which supports an increased catalase activity in lapachol-treated cells. Survival assays under aerobic and microaerophilic conditions could further link lapachol toxicity to increased ROS formation under aerobic conditions in *S. aureus*. The survival of lapachol-treated *S. aureus* cells was strongly increased under microaerophilic conditions, while the aerobic culture was protected against lapachol toxicity by the ROS scavenger N-acetyl cysteine. These combined results of an oxidative shift in E_{BSH}, elevated H_2O_2 levels with the Tpx-roGFP2 biosensor, faster H_2O_2 detoxification and increased survival with decreased ROS levels indicate that the redox-cycling mode is the main antimicrobial mode of action of lapachol in *S. aureus* cells.

In agreement with the oxidative mode, growth and survival assays revealed an increased sensitivity of the *katA* mutant to lapachol, which is compromised in H_2O_2 detoxification [72]. Apart from *katA*, the peroxidase *ahpCF* operon is very strongly 20-26-fold induced by lapachol. Both KatA and AhpCF have compensatory roles in peroxide detoxification, since the absence of KatA resulted in elevated AhpCF expression and *vice versa* [72]. Our transcriptome results indicate that

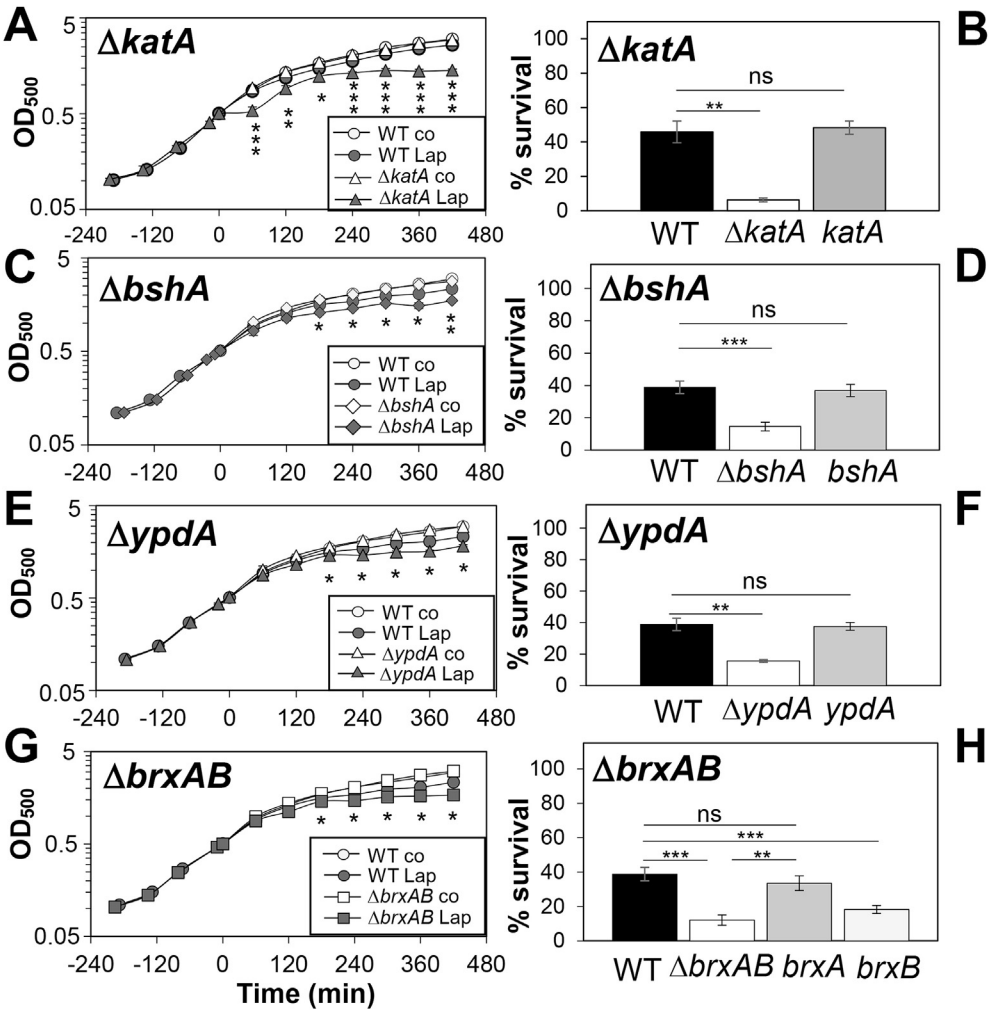

Fig. 7. The *S. aureus katA, bshA, ypdA* and *brxAB* deletion mutants are more sensitive under lapachol stress as shown in growth and survival assays. (A–H) Growth curves **(A, C, E, G)** and survival assays **(B,D,F,H)** were performed of *S. aureus* COL WT, *katA*, *bshA*, *brxAB*, and *ypdA* mutants and complemented strains (*katA*, *bshA, ypdA, brxA, brxB*) in RPMI medium after exposure to lapachol stress at an OD_{500} of 0.5. Growth phenotypes were determined after 300 μM lapachol and survival rates were calculated 4 h after exposure to 400 μM lapachol and determination of CFUs. Growth curves of the *bshA, katA, ypdA, brxA* and *brxB* complemented strains are shown in Fig. S3. Survival of the untreated control was set to 100%. Mean values and SD of four biological replicates are presented. The statistics was calculated using a Student's unpaired two-tailed *t*-test by the graph prism software. Symbols are: $^{ns}p > 0.05$, $^{*}p \leq 0.05$, $^{**}p \leq 0.01$ and $^{***}p \leq 0.001$.

both KatA and AhpCF are highly induced by lapachol to remove H_2O_2. The increased catalase activity was confirmed using the FOX assay in extracts of lapachol-treated cells. In the *katA* mutant, the *ahpCF* operon might compensate for detoxification of H_2O_2 which is produced by lapachol.

In addition, we analyzed the thiol-oxidation of GapDH and the HypR repressor in the proteome of *S. aureus*. Lapachol induced *S*-bacillithiolation of GapDH both *in vivo* and *in vitro*, supporting further ROS generation. *S*-bacillithiolation of GapDH was previously observed in response to strong oxidants, such as HOCl and by the antimicrobial coating AGXX®, which causes hydroxyl radical formation [48,59]. Thus, the previously measured hydroxyperoxyl radical under lapachol stress might provoke *S*-bacillithiolation of GapDH [24]. Regeneration of *S*-bacillithiolated proteins and BSSB was shown to require the BrxA/BSH/YpdA pathway in *S. aureus*, which is important under oxidative stress and infections [48,51,52]. Consistent with these results, the *bshA*, *brxAB* and *ypdA* mutants showed significant growth and survival defects under lapachol stress. This confirms the importance of the BrxA/BSH/YpdA pathway for recovery of *S. aureus* from lapachol stress by reduction of oxidized proteins and BSSB.

The HypR repressor was previously shown to sense strong disulfide stress, such as HOCl, AGXX® and allicin [41,59,65]. The redox-sensing mechanism of HypR involves intermolecular disulfide formation under HOCl stress. Here, we confirmed that HypR is oxidized to the HypR disulfide-linked dimer leading to its inactivation and derepression of transcription of the disulfide reductase-encoding *merA* gene. Consistent with these results, the *hypR-merA* operon was 5-fold induced in the transcriptome under lapachol stress. The increased protein thiol-oxidation by lapachol is further in agreement with the strong induction of the CtsR and HrcA regulons, controlling Clp proteases and the DnaK-GrpE, GroESL chaperones to degrade and refold oxidatively damaged proteins. Altogether, our results indicate that lapachol provokes mainly an oxidative stress response in the transcriptome, which was confirmed by an oxidized E_{BSH}, elevated H_2O_2 levels, increased catalase activity and protein thiol-oxidation during aerobic growth in *S. aureus*.

However, quinones have been described to exert their cytotoxicity via oxidative and electrophilic mechanisms [13,27,28]. In the electrophilic mode, quinones lead to *S*-alkylation of nucleophilic Cys residues, resulting in irreversible protein aggregation and depletion of Cys proteins in the proteome [29]. Thus, the question arises whether the naphthoquinone lapachol could lead to thiol-*S*-alkylation and aggregation of protein thiols. Previous studies on diesel exhaust phenanthraquinone revealed the oxidation of proximal protein thiols and oxidative modification of Cu, Zn superoxide dismutase through the redox cycling mode of action [33,73]. Our transcriptome signature revealed the induction of the quinone-specific MhqR and QsrR regulons under lapachol stress, which could point to the alkylation mode. However, these quinone-specific regulons were induced at lower levels (~10-fold) compared to the oxidant-induced PerR-regulated *ahpCF* and *katA* genes. This might indicate that the naphthoquinone lapachol does not lead to alkylation and aggregation of protein thiols as shown for benzoquinones previously [29]. In contrast, the MhqR and QsrR regulons responded much stronger to the hydroquinone MHQ in previous transcriptome studies [26]. Specifically, MHQ leads to 34-67-fold induction of the MhqR regulon and up-to 280-fold induction of the QsrR regulon in *S. aureus* [26]. The *S*-alkylation and oxidation modes of

action were both previously demonstrated for benzoquinones in *B. subtilis* [29].

To exclude the alkylation mode of lapachol, we treated the GapDH protein with increasing concentrations of lapachol up-to 7.5 mM *in vitro*, but did not observe any aggregation in the higher molecular range (Fig. S1A) compared to previous studies with benzoquinones [29]. The isolation of the insoluble protein fraction in cell extracts *in vivo* did not reveal increased protein aggregates after treatment of cells with 0.3 and 1 mM lapachol (Fig. S1B). In addition, no irreversible protein aggregation could be observed for the HypR repressor, which was oxidized to the reversible HypR intermolecular disulfides indicative for the oxidative mode (Fig. S2AB). We did not find any evidence for protein alkylation and aggregation since cellular proteins could be well separated using SDS-PAGE. No alkylated aggregates migrated in the upper range of the SDS gel or remained in the stacking gel (see loading controls of Fig. 6A and Fig. S2AB) as observed previously for benzoquinones [29]. These results were expected since the quinone ring is fully substituted in lapachol, which prevents thiol-*S*-alkylation and aggregation of protein thiols [27,34]. In general, the toxicity and alkylation activity increases with the number of unsubstituted positions adjacent to the keto groups of the quinone rings [27,34]. In conclusion, our results demonstrate that lapachol leads to ROS formation and acts mainly via its redox-cycling oxidative mode as antimicrobial mechanism in *S. aureus*.

Finally, the question arises if *S. aureus* is able to detoxify lapachol. Lapachol metabolic pathways have been studied in fungi and streptomycetes, which involve monooxygenases or dioxygenases [74,75]. Our transcriptome data identified the flavohemoglobin *hmp* as strongly induced under lapachol stress in *S. aureus*. Hmp was characterized as NO dioxygenase, which converts NO and O_2 to NO_3^- via the haem-Fe^{2+} active center using NADPH and FAD as cofactors for electron transfer [68]. Recently, *S. aureus* Hmp was revealed to function in detoxification of quinones by mixed single and two-electron reduction mechanisms with preference for 1,4-naphthoquinones as best electron acceptors [69]. Quinone reduction required electrons from NADH and reduced FAD, but not from haem-$Fe^{2+}O_2$, indicating that quinones are subverse substrates for Hmp using different mechanisms for detoxification compared to NO [69]. These results indicate that lapachol detoxification could involve various NADPH-dependent flavoenzymes in *S. aureus*, which are upregulated in the transcriptome under lapachol stress and remain to be subjects of future studies.

Acknowledgements

This work was supported by an ERC Consolidator grant (GA 615585) MYCOTHIOLOME and grants from the Deutsche Forschungsgemeinschaft (AN746/4-1 and AN746/4-2) within the SPP1710, by the SFB973 project C08N and by the SFB/TR84 project B06 to H.A.

Appendix A. Supplementary data

Supplementary data to this article can be found online at https://doi.org/10.1016/j.freeradbiomed.2020.07.025.

References

[1] F.D. Lowy, *Staphylococcus aureus* infections, N. Engl. J. Med. 339 (8) (1998) 520–532.
[2] H.W. Boucher, G.R. Corey, Epidemiology of methicillin-resistant *Staphylococcus aureus*, Clin. Infect. Dis. 46 (Suppl 5) (2008) S344–S349.
[3] G.L. Archer, *Staphylococcus aureus*: a well-armed pathogen, Clin. Infect. Dis. 26 (5) (1998) 1179–1181.
[4] S.Y. Tong, J.S. Davis, E. Eichenberger, T.L. Holland, V.G. Fowler Jr., *Staphylococcus aureus* infections: epidemiology, pathophysiology, clinical manifestations, and management, Clin. Microbiol. Rev. 28 (3) (2015) 603–661.
[5] D.M. Livermore, Antibiotic resistance in staphylococci, Int. J. Antimicrob. Agents 16 (Suppl 1) (2000) S3–S10.
[6] S. Lakhundi, K. Zhang, Methicillin-Resistant *Staphylococcus aureus*: molecular characterization, evolution, and epidemiology, Clin. Microbiol. Rev. 31 (4) (2018).
[7] V.D. Nguyen, C. Wolf, U. Mäder, M. Lalk, P. Langer, U. Lindequist, M. Hecker, H. Antelmann, Transcriptome and proteome analyses in response to 2-methylhydroquinone and 6-brom-2-vinyl-chroman-4-on reveal different degradation systems involved in the catabolism of aromatic compounds in *Bacillus subtilis*, Proteomics 7 (9) (2007) 1391–1408.
[8] K.R. Vann, G. Ekiz, S. Zencir, E. Bedir, Z. Topcu, N. Osheroff, Effects of secondary metabolites from the fungus *Septofusidium berolinense* on DNA cleavage mediated by human topoisomerase II alpha, Chem. Res. Toxicol. 29 (3) (2016) 415–420.
[9] G. Ekiz, E.E. Hames, A. Nalbantsoy, E. Bedir, Two rare quinone-type metabolites from the fungus *Septofusidium berolinense* and their biological activities, J. Antibiot. (Tokyo) 69 (2) (2016) 111–113.
[10] H. Hussain, I.R. Green, Lapachol and lapachone analogs: a journey of two decades of patent research(1997-2016), Expert Opin. Ther. Pat. 27 (10) (2017) 1111–1121.
[11] C.A. Colwell, M. McCall, Studies on the mechanism of antibacterial action of 2-methyl-1,4-naphthoquinone, Science 101 (2632) (1945) 592–594.
[12] H. Schildknecht, Die Wehrchemie von Land- und Wasserkäfern, Angew. Chem. 82 (1) (1970) 17–25.
[13] R.A. Morton, Biochemistry of Quinones, Academic Press, 1965.
[14] Á. Ravelo, A. Estévez-Braun, E. Pérez-Sacau, The Chemistry and Biology of Lapachol and Related Natural Products α and β-lapachones, Studies in Natural Products Chemistry, Elsevier, 2003, pp. 719–760.
[15] F. Epifano, S. Genovese, S. Fiorito, V. Mathieu, R. Kiss, Lapachol and its congeners as anticancer agents: a review, Phytochemistry Rev. 13 (1) (2014) 37–49.
[16] O.A. Binutu, K.E. Adesogan, J.I. Okogun, Antibacterial and antifungal compounds from *Kigelia pinnata*, Planta Med. 62 (4) (1996) 352–353.
[17] R.M. Ali, P.J. Houghton, A. Raman, J.R.S. Hoult, Antimicrobial and antiinflammatory activities of extracts and constituents of *Oroxylum indicum* (L.) Vent, Phytomedicine 5 (5) (1998) 375–381.
[18] B.S. Park, J.R. Kim, S.E. Lee, K.S. Kim, G.R. Takeoka, Y.J. Ahn, J.H. Kim, Selective growth-inhibiting effects of compounds identified in *Tabebuia impetiginosa* inner bark on human intestinal bacteria, J. Agric. Food Chem. 53 (4) (2005) 1152–1157.
[19] E.M. Pereira, B. Machado Tde, I.C. Leal, D.M. Jesus, C.R. Damaso, A.V. Pinto, M. Giambiagi-deMarval, R.M. Kuster, K.R. Santos, *Tabebuia avellanedae* naphthoquinones: activity against methicillin-resistant staphylococcal strains, cytotoxic activity and in vivo dermal irritability analysis, Ann. Clin. Microbiol. Antimicrob. 5 (2006) 5.
[20] M.A. Souza, S. Johann, L.A. Lima, F.F. Campos, I.C. Mendes, H. Beraldo, E.M. Souza-Fagundes, P.S. Cisalpino, C.A. Rosa, T.M. Alves, N.P. de Sa, C.L. Zani, The antimicrobial activity of lapachol and its thiosemicarbazone and semicarbazone derivatives, Mem. Inst. Oswaldo Cruz 108 (3) (2013).
[21] E. Perez-Sacau, R.G. Diaz-Penate, A. Estevez-Braun, A.G. Ravelo, J.M. Garcia-Castellano, L. Pardo, M. Campillo, Synthesis and pharmacophore modeling of naphthoquinone derivatives with cytotoxic activity in human promyelocytic leukemia HL-60 cell line, J. Med. Chem. 50 (4) (2007) 696–706.
[22] S.N. Sunassee, C.G. Veale, N. Shunmoogam-Gounden, O. Osoniyi, D.T. Hendricks, M.R. Caira, J.A. de la Mare, A.L. Edkins, A.V. Pinto, E.N. da Silva Junior, M.T. Davies-Coleman, Cytotoxicity of lapachol, beta-lapachone and related synthetic 1,4-naphthoquinones against oesophageal cancer cells, Eur. J. Med. Chem. 62 (2013) 98–110.
[23] M.N. Rocha, P.M. Nogueira, C. Demicheli, L.G. de Oliveira, M.M. da Silva, F. Frezard, M.N. Melo, R.P. Soares, Cytotoxicity and in vitro antileishmanial activity of antimony (V), bismuth (V), and tin (IV) complexes of lapachol, Bioinorgan. Chem. Appl. 2013 (2013) 961783.
[24] M.O. Goulart, P. Falkowski, T. Ossowski, A. Liwo, Electrochemical study of oxygen interaction with lapachol and its radical anions, Bioelectrochemistry 59 (1–2) (2003) 85–87.
[25] Y. Kumagai, Y. Tsurutani, M. Shinyashiki, S. Homma-Takeda, Y. Nakai, T. Yoshikawa, N. Shimojo, Bioactivation of lapachol responsible for DNA scission by NADPH-cytochrome P450 reductase, Environ. Toxicol. Pharmacol. 3 (4) (1997) 245–250.
[26] V.N. Fritsch, V.V. Loi, T. Busche, A. Sommer, K. Tedin, D.J. Nürnberg, J. Kalinowski, J. Bernhardt, M. Fulde, H. Antelmann, The MarR-type repressor MhqR confers quinone and antimicrobial resistance in *Staphylococcus aureus*, Antioxidants Redox Signal. 31 (16) (2019) 1235–1252.
[27] P.J. O'Brien, Molecular mechanisms of quinone cytotoxicity, Chem. Biol. Interact. 80 (1) (1991) 1–41.
[28] T.J. Monks, R.P. Hanzlik, G.M. Cohen, D. Ross, D.G. Graham, Quinone chemistry and toxicity, Toxicol. Appl. Pharmacol. 112 (1) (1992) 2–16.
[29] M. Liebeke, D.C. Pöther, N. van Duy, D. Albrecht, D. Becher, F. Hochgräfe, M. Lalk, M. Hecker, H. Antelmann, Depletion of thiol-containing proteins in response to quinones in *Bacillus subtilis*, Mol. Microbiol. 69 (6) (2008) 1513–1529.
[30] H. Antelmann, J.D. Helmann, Thiol-based redox switches and gene regulation, Antioxidants Redox Signal. 14 (6) (2011) 1049–1063.
[31] V.V. Loi, M. Rossius, H. Antelmann, Redox regulation by reversible protein S-thiolation in bacteria, Front. Microbiol. 6 (2015) 187.
[32] S. Bittner, When quinones meet amino acids: chemical, physical and biological consequences, Amino Acids 30 (3) (2006) 205–224.
[33] Y. Kumagai, S. Koide, K. Taguchi, A. Endo, Y. Nakai, T. Yoshikawa, N. Shimojo, Oxidation of proximal protein sulfhydryls by phenanthraquinone, a component of diesel exhaust particles, Chem. Res. Toxicol. 15 (4) (2002) 483–489.
[34] M.T. Smith, Quinones as mutagens, carcinogens, and anticancer agents: introduction and overview, J. Toxicol. Environ. Health 16 (5) (1985) 665–672.
[35] T.W. Schultz, G.D. Sinks, M.T.D. Cronin, Quinone-induced toxicity to Tetrahymena: structure-activity relationships, Aquat. Toxicol. 39 (3–4) (1997) 267–278.

[36] A. Brunmark, E. Cadenas, Redox and addition chemistry of quinoid compounds and its biological implications, Free Radic. Biol. Med. 7 (4) (1989) 435–477.
[37] Q. Ji, L. Zhang, M.B. Jones, F. Sun, X. Deng, H. Liang, H. Cho, P. Brugarolas, Y.N. Gao, S.N. Peterson, Molecular mechanism of quinone signaling mediated through S-quinonization of a YodB family repressor QsrR, Proc. Natl. Acad. Sci. Unit. States Am. 110 (13) (2013) 5010–5015.
[38] C.J. Ji, J.H. Kim, Y.B. Won, Y.E. Lee, T.W. Choi, S.Y. Ju, H. Youn, J.D. Helmann, J.W. Lee, *Staphylococcus aureus* PerR is a hypersensitive hydrogen peroxide sensor using iron-mediated histidine oxidation, J. Biol. Chem. 290 (33) (2015) 20374–20386.
[39] A. Pinochet-Barros, J.D. Helmann, Redox sensing by Fe(2+) in bacterial Fur family metalloregulators, Antioxidants Redox Signal. 29 (18) (2018) 1858–1871.
[40] M.J. Horsburgh, M.O. Clements, H. Crossley, E. Ingham, S.J. Foster, PerR controls oxidative stress resistance and iron storage proteins and is required for virulence in *Staphylococcus aureus*, Infect. Immun. 69 (6) (2001) 3744–3754.
[41] V.V. Loi, T. Busche, K. Tedin, J. Bernhardt, J. Wollenhaupt, N.T.T. Huyen, C. Weise, J. Kalinowski, M.C. Wahl, M. Fulde, H. Antelmann, Redox-sensing under hypochlorite stress and infection conditions by the Rrf2-family repressor HypR in *Staphylococcus aureus*, Antioxidants Redox Signal. 29 (7) (2018) 615–636.
[42] P. Chandrangsu, V.V. Loi, H. Antelmann, J.D. Helmann, The role of bacillithiol in Gram-positive firmicutes, Antioxidants Redox Signal. 28 (6) (2018) 445–462.
[43] G.L. Newton, R.C. Fahey, M. Rawat, Detoxification of toxins by bacillithiol in *Staphylococcus aureus*, Microbiology 158 (Pt 4) (2012) 1117–1126.
[44] D.C. Pöther, P. Gierok, M. Harms, J. Mostertz, F. Hochgräfe, H. Antelmann, C.J. Hamilton, I. Borovok, M. Lalk, Y. Aharonowitz, M. Hecker, Distribution and infection-related functions of bacillithiol in *Staphylococcus aureus*, Int J Med Microbiol 303 (3) (2013) 114–123.
[45] A.C. Posada, S.L. Kolar, R.G. Dusi, P. Francois, A.A. Roberts, C.J. Hamilton, G.Y. Liu, A. Cheung, Importance of bacillithiol in the oxidative stress response of *Staphylococcus aureus*, Infect. Immun. 82 (1) (2014) 316–332.
[46] B.K. Chi, K. Gronau, U. Mäder, B. Hessling, D. Becher, H. Antelmann, S-bacillithiolation protects against hypochlorite stress in *Bacillus subtilis* as revealed by transcriptomics and redox proteomics, Mol. Cell. Proteomics 10 (11) (2011) M111 009506.
[47] B.K. Chi, A.A. Roberts, N.T.T. Huyen, K. Bäsell, D. Becher, D. Albrecht, C.J. Hamilton, H. Antelmann, S-bacillithiolation protects conserved and essential proteins against hypochlorite stress in firmicutes bacteria, Antioxidants Redox Signal. 18 (11) (2013) 1273–1295.
[48] M. Imber, N.T.T. Huyen, A.J. Pietrzyk-Brzezinska, V.V. Loi, M. Hillion, J. Bernhardt, L. Thärichen, K. Kolsek, M. Saleh, C.J. Hamilton, L. Adrian, F. Gräter, M.C. Wahl, H. Antelmann, Protein S-bacillithiolation functions in thiol protection and redox regulation of the glyceraldehyde-3-phosphate dehydrogenase Gap in *Staphylococcus aureus* under hypochlorite stress, Antioxidants Redox Signal. 28 (6) (2018) 410–430.
[49] M. Imber, V.V. Loi, S. Reznikov, V.N. Fritsch, A.J. Pietrzyk-Brzezinska, J. Prehn, C. Hamilton, M.C. Wahl, A.K. Bronowska, H. Antelmann, The aldehyde dehydrogenase AldA contributes to the hypochlorite defense and is redox-controlled by protein S-bacillithiolation in *Staphylococcus aureus*, Redox Biol 15 (2018) 557–568.
[50] M. Imber, A.J. Pietrzyk-Brzezinska, H. Antelmann, Redox regulation by reversible protein S-thiolation in Gram-positive bacteria, Redox Biol 20 (2018) 130–145.
[51] N. Linzner, V.V. Loi, V.N. Fritsch, Q.N. Tung, S. Stenzel, M. Wirtz, R. Hell, C.J. Hamilton, K. Tedin, M. Fulde, H. Antelmann, *Staphylococcus aureus* uses the bacilliredoxin (BrxAB)/bacillithiol disulfide reductase (YpdA) redox pathway to defend against oxidative stress under infections, Front. Microbiol. 10 (2019) 1355.
[52] I.V. Mikheyeva, J.M. Thomas, S.L. Kolar, A.R. Corvaglia, N. Gaiotaa, S. Leo, P. Francois, G.Y. Liu, M. Rawat, A.L. Cheung, YpdA, a putative bacillithiol disulfide reductase, contributes to cellular redox homeostasis and virulence in *Staphylococcus aureus*, Mol. Microbiol. 111 (4) (2019) 1039–1056.
[53] A. Gaballa, B.K. Chi, A.A. Roberts, D. Becher, C.J. Hamilton, H. Antelmann, J.D. Helmann, Redox regulation in *Bacillus subtilis*: the bacilliredoxins BrxA(YphP) and BrxB(YqiW) function in de-bacillithiolation of S-bacillithiolated OhrR and MetE, Antioxidants Redox Signal. 21 (3) (2014) 357–367.
[54] V.V. Loi, M. Harms, M. Müller, N.T.T. Huyen, C.J. Hamilton, F. Hochgräfe, J. Pane-Farre, H. Antelmann, Real-time imaging of the bacillithiol redox potential in the human pathogen *Staphylococcus aureus* using a genetically encoded bacilliredoxin-fused redox biosensor, Antioxidants Redox Signal. 26 (15) (2017) 835–848.
[55] V. Van Loi, H. Antelmann, Method for measurement of bacillithiol redox potential changes using the Brx-roGFP2 redox biosensor in *Staphylococcus aureus*, Methods (Orlando) 7 (2020) 100900.
[56] M. Arnaud, A. Chastanet, M. Debarbouille, New vector for efficient allelic replacement in naturally nontransformable, low-GC-content, gram-positive bacteria, Appl. Environ. Microbiol. 70 (11) (2004) 6887–6891.
[57] E.D. Rosenblum, S. Tyrone, Serology, density, and morphology of staphylococcal phages, J. Bacteriol. 88 (6) (1964) 1737–1742.
[58] R. Brückner, E. Wagner, F. Götz, Characterization of a sucrase gene from *Staphylococcus xylosus*, J. Bacteriol. 175 (3) (1993) 851–857.
[59] V.V. Loi, T. Busche, T. Preuss, J. Kalinowski, J. Bernhardt, H. Antelmann, The AGXX® antimicrobial coating causes a thiol-specific oxidative stress response and protein S-bacillithiolation in *Staphylococcus aureus*, Front. Microbiol. 9 (2018) 3037.
[60] M.I. Love, W. Huber, S. Anders, Moderated estimation of fold change and dispersion for RNA-seq data with DESeq2, Genome Biol. 15 (12) (2014) 550.
[61] R. Hilker, K.B. Stadermann, O. Schwengers, E. Anisiforov, S. Jaenicke, B. Weisshaar, T. Zimmermann, A. Goesmann, ReadXplorer 2-detailed read mapping analysis and visualization from one single source, Bioinformatics 32 (24) (2016) 3702–3708.
[62] J. Nourooz-Zadeh, J. Tajaddini-Sarmadi, S.P. Wolff, Measurement of plasma hydroperoxide concentrations by the ferrous oxidation-xylenol orange assay in conjunction with triphenylphosphine, Anal. Biochem. 220 (2) (1994) 403–409.
[63] B. Groitl, J.U. Dahl, J.W. Schroeder, U. Jakob, *Pseudomonas aeruginosa* defense systems against microbicidal oxidants, Mol. Microbiol. 106 (3) (2017) 335–350.
[64] T. Tomoyasu, F. Arsene, T. Ogura, B. Bukau, The C terminus of sigma(32) is not essential for degradation by FtsH, J. Bacteriol. 183 (20) (2001) 5911–5917.
[65] V.V. Loi, N.T.T. Huyen, T. Busche, Q.N. Tung, M.C.H. Gruhlke, J. Kalinowski, J. Bernhardt, A.J. Slusarenko, H. Antelmann, *Staphylococcus aureus* responds to allicin by global S-thioallylation - role of the Brx/BSH/YpdA pathway and the disulfide reductase MerA to overcome allicin stress, Free Radic. Biol. Med. 139 (2019) 55–69.
[66] D. Frees, U. Gerth, H. Ingmer, Clp chaperones and proteases are central in stress survival, virulence and antibiotic resistance of *Staphylococcus aureus*, Int J Med Microbiol 304 (2) (2014) 142–149.
[67] D. Frees, K. Savijoki, P. Varmanen, H. Ingmer, Clp ATPases and ClpP proteolytic complexes regulate vital biological processes in low GC, Gram-positive bacteria, Mol. Microbiol. 63 (5) (2007) 1285–1295.
[68] R.K. Poole, Flavohaemoglobin: the Pre-eminent Nitric Oxide-Detoxifying Machine of Microorganisms vol. 9, (2020), p. F1000Res.
[69] M. Moussaoui, L. Miseviciene, Z. Anusevicius, A. Maroziene, F. Lederer, L. Baciou, N. Cenas, Quinones and nitroaromatic compounds as subversive substrates of *Staphylococcus aureus* flavohemoglobin, Free Radic. Biol. Med. 123 (2018) 107–115.
[70] M. Falord, U. Mäder, A. Hiron, M. Debarbouille, T. Msadek, Investigation of the *Staphylococcus aureus* GraSR regulon reveals novel links to virulence, stress response and cell wall signal transduction pathways, PloS One 6 (7) (2011) e21323.
[71] C.G. Oliveira, F.F. Miranda, V.F. Ferreira, C.C. Freitas, R.F. Rabello, J.M. Carballido, L.C. Corrêa, Synthesis and antimicrobial evaluation of 3-hydrazino-naphthoquinones as analogs of lapachol, J. Braz. Chem. Soc. 12 (3) (2001) 339–345.
[72] K. Cosgrove, G. Coutts, I.M. Jonsson, A. Tarkowski, J.F. Kokai-Kun, J.J. Mond, S.J. Foster, Catalase (KatA) and alkyl hydroperoxide reductase (AhpC) have compensatory roles in peroxide stress resistance and are required for survival, persistence, and nasal colonization in *Staphylococcus aureus*, J. Bacteriol. 189 (3) (2007) 1025–1035.
[73] R. Koizumi, K. Taguchi, M. Hisamori, Y. Kumagai, Interaction of 9,10-phenanthraquinone with dithiol causes oxidative modification of Cu,Zn-superoxide dismutase (SOD) through redox cycling, J. Toxicol. Sci. 38 (3) (2013) 317–324.
[74] S. Otten, J.P. Rosazza, Microbial transformations of natural antitumor agents: oxidation of lapachol by *Penicillium notatum*, Appl. Environ. Microbiol. 35 (3) (1978) 554–557.
[75] S.L. Otten, J.P. Rosazza, Oxidative ring fission of the naphthoquinones lapachol and dichloroallyl lawsone by *Penicillium notatum*, J. Biol. Chem. 258 (3) (1983) 1610–1613.